Published in final edited form as:
Cell Host Microbe. 2011 March 17; 9(3): 212–222. doi:10.1016/j.chom.2011.02.006.

Hypomorphic mutation in the site-1 protease *Mbtps1* endows resistance to persistent viral infection in a cell specific manner

Daniel L. Popkin[1,2], **John R. Teijaro**[1], **Brian M. Sullivan**[1], **Shuzo Urata**[1], **Sophie Rutschmann**[2], **Juan Carlos de la Torre**[1], **Stefan Kunz**[3], **Bruce Beutler**[2,*], and **Michael Oldstone**[1,*]

[1] Department of Immunology and Microbial Sciences, The Scripps Research Institute, 10550 North Torrey Pines Road, La Jolla, CA 92037, USA

[2] Department of Genetics, The Scripps Research Institute, 10550 North Torrey Pines Road, La Jolla, CA 92037, USA

SUMMARY

The prototypic arenavirus lymphocytic choriomeningitis virus (LCMV), which naturally persists in rodents, represents a model for HIV, HBV and HCV. Cleavage of the viral glycoprotein precursor by membrane-bound transcription factor peptidase, site 1 (Mbtps1 or Site-1 Protease) is crucial for the life cycle of arenaviruses and therefore represents a potential target for therapy. Recently we reported a viable hypomorphic allele of Mbtps1 (*woodrat*), encoding a protease with diminished enzymatic activity. Using the *woodrat* allele, we examine the role of Mbtps1 during persistent LCMV infection. Surprisingly, Mbtps1 inhibition limits persistent but not acute viral infection and is associated with an organ/cell type specific decrease in viral titers. Analysis of bone marrow-derived dendritic cells from *woodrat* mice supports their specific role in resolving persistent viral infection. These results support *in vivo* targeting of Mbtps1 in the treatment of arenavirus infections, and demonstrate a critical role for dendritic cells in persistent viral infections.

Keywords

persistent infection; Mbtps1; Site-1 protease; HIV; Hepatitis B; Hepatitis C; lymphocytic choriomeningitis virus; dendritic cells; immunotherapy; arenavirus

INTRODUCTION

Membrane-bound transcription factor peptidase, site 1 (Mbtps1), also known as Site-1 Protease (S1P), cleaves several host and viral proteins. Host cell substrates include S1P itself, b-ZIP transcription factors such as the sterol regulatory element binding proteins (SREBP1 and SREBP2), ATF6, CREBH, CREB4, OASIS and Luman(Chen et al., 2002; Nadanaka et al., 2004; Ye et al., 2000). Cleavage of the SREBP transcription factors permits

Correspondence to: Daniel L. Popkin.

[3]Current address: Institute of Microbiology, University Hospital Center and University of Lausanne, Lausanne, Switzerland.
[*]These authors contributed equally to the work.

nuclear translocation and expression of genes required for the synthesis and uptake of cholesterol (Brown et al., 2000). Cleavage of ATF6 mediates one aspect of the unfolded protein response (UPR), by inducing expression of Grp78(BiP) and Grp94 which encode key chaperones required for the UPR (Ron and Walter, 2007). Viral glycoproteins are also a target of S1P. Cleavage of the glycoprotein precursor (GPC), is a crucial step in the life cycle of all major human pathogenic arenaviruses including lymphocytic choriomeningitis virus (LCMV) and Lassa hemorrhagic fever virus as well as for the bunyavirus Crimean-Congo hemorrhagic fever virus(Bergeron et al., 2007; Rojek et al., 2010). In the course of evolution, these viruses have seized upon the catalytic activity of S1P and its location in the endoplasmic reticulum and Golgi apparatus to process their envelope glycoproteins. Processing of the GPC by S1P is necessary for cell-to-cell propagation of infection and production of infectious virus in S1P deficient cells *in vitro* (Rojek et al., 2010). The consequences of complete deficiency of S1P *in vivo* cannot be assessed, because the knockout allele is embryonic lethal in homozygous form(Yang et al., 2001). Recently we reported a viable hypomorphic allele of Mbtps1 (*woodrat; wrt*), encoding a S1P protein with diminished enzymatic activity. *Wrt* homozygotes are less likely to survive to birth, and are prone to dextran sulfate sodium-induced colitis by virtue of their defective UPR (Brandl et al., 2009). The wrt/- genotype is lethal *in utero*, suggesting that the hypomorphic effect of the mutation is relatively severe.

Here, we have tested the effects of the *wrt* mutation on resistance to the prototypic Arenavirus family member, lymphocytic choromeningitis virus (LCMV). We find that persistent viral infection is impossible in the context of restricted S1P activity, and infer a critical role for bone marrow derived dendritic cells (bmDC) in the maintenance of persistence.

RESULTS

woodrat Mice are Resistant to Persistent LCMV Clone13 Infection

Site 1 Protease (S1P) is required for arenavirus life cycle *in vitro* (Rojek and Kunz, 2008). Therefore we hypothesized that C57BL/6J mice homozygous for the hypomorphic *Mbtps1*^{wrt} allele (Brandl et al., 2009), would be resistant to arenaviral challenge. However, our original studies with the acute strain of the prototypic arenavirus, lymphocytic choriomeningitis virus Armstrong strain (LCMV Arm) showed no striking defects in viral growth kinetics *in vitro* or *in vivo* (Figs. 1A,2A, 4A). Given the critical role of *Mbtps1* in arenavirus growth and our knowledge that proteolytic activity was functionally compromised in some tissues (Brandl et al., 2009) we hypothesized that a persistent variant of LCMV Arm, LCMV Clone 13 (Cl13), that infects a distinct set of target cells compared with LCMV Arm would exhibit altered *in vivo* growth. Only 2 amino acids distinguish the acute LCMV Arm virus from persistent LCMV Cl13 virus. Our lab and others have shown that these differing residues do not lie within immunodominant epitopes that engage the critical cytotoxic CD8+ T cell response required for viral clearance. Instead, these two residues affect viral tropism which is thought to be the primary variable resulting in viral persistence versus acute viral clearance (Sevilla et al., 2000; Sevilla et al., 2004a). Although LCMV Arm is completely cleared by the host immune response within 2 weeks, LCMV Cl13 maintains high levels of viremia for 2–3 months followed by extended or even life-long viral persistence in the kidney (de la Torre and Oldstone, 1996; Oldstone, 2002; Recher et al., 2007). Interestingly, we could not detect LCMV Cl13 in tissues examined at 3 weeks post infection in *Mbtps1*^{wrt}, as observed in infections by the acute LCMV Arm strain (Figure 2A).

woodrat Mice Clear a Normally Persistent Virus Despite Being Immunodeficient

LCMV persistence relies on replication during an ongoing host immune response. We hypothesized that *wrt* host resistance was largely due to defective viral replication in bmDCs and perhaps other cell types secondary to defective GP processing. However, host resistance might also be due to an augmented anti-viral immune response. Therefore, we directly measured the dominant effectors in LCMV clearance (Jamieson et al., 1987; Li et al., 2009; van der Most et al., 1996) focusing on the T and B lymphocyte responses. We measured both the numbers and function of viral antigen specific lymphocyte responses in *wrt* versus WT controls (Table I and Figure 1BC). By enumerating viral antigen specific T cells, and measuring their effector function as indicated by cytokine production and direct *ex vivo* killing by CD8 cells, as well as specific antibody responses *in vivo*, we found that *wrt* immune responses were diminished compared to WT controls in the first week of infection (Table I, Figure 1BC). However, as *wrt* do clear the normally persistent LCMV Cl13 we reasoned that their residual immune response must be sufficient to eliminate infected cells. Consistent with this hypothesis, we observed an augmented immune response in *wrt* T cells 9 dpi in comparison to the otherwise “exhausted” response normally found in persistently LCMV Cl13 infected WT animals (Figure 1DE).

woodrat Resistance is not Reversed with Cholesterol Supplementation

To find alternative explanations for the protective effect of the *wrt* mutation, we supplemented mice with a 5% cholesterol diet (sufficient to partially restore *wrt* T cell immune deficiency, Table I) and challenged them with LCMV Cl13. Given the important requirement of cholesterol in both the viral life cycle and host immune responses (Bukrinsky and Sviridov, 2006;Riethmüller et al., 2006;Rojek et al., 2008), we hypothesized that limiting amounts of cholesterol were responsible for *wrt* resistance. However, cholesterol repletion did not revert *wrt* resistance (Figure S1A). As another possibility, we assessed whether type I interferon production might partially explain *wrt* resistance. However the increase in IFNalpha which we observed did not meet statistical significance (Figure S1B) and its mechanistic contribution is unclear at this time.

Defective LCMV Cl13 Establishment in Bone Marrow and Kidney

As tropism is thought to be one of the key factors distinguishing viral clearance versus persistence, we examined the kinetics of viral replication in several organs (Figure 2A). Surprisingly, we found normal establishment of viral infection in spleen and liver 5 dpi. However, acutely high viral loads in bone marrow and kidney were not observed after LCMV Cl13 infection of *Mbtps1*^{wrt} homozygotes (Figure 2A) at this time point. Resistance is observed in both tissues despite the presence of high levels of infectious virus in the blood. However at 9 dpi, similar levels of LCMV Cl13 were found in the kidneys of WT and *wrt* mice. However, no appreciable amount of infectious virus nor viral antigen was detected in the bone marrow of *Mbtps1*^{wrt} at any time (Figure 2AB).

Recent work has implicated bone marrow in establishing persistent viral infection (Carter et al., 2010) and more specifically dendritic cells (DCs) and their progenitors are thought to be critical for persistent viral infections including LCMV Cl13 (Sevilla et al., 2003; Sevilla et al., 2004a). Thus we further analyzed viral replication in the bone marrow of *Mbtps1*^{wrt} homozygotes. We analyzed bone marrow cells utilizing flow cytometry and found that both *Mbtps1*$^{wrt/wrt}$ DCs and their monocyte precursors were resistant to LCMV Cl13 infection (Figure 2B). This is specific to the bone marrow environment as *Mbtps1*$^{wrt/wrt}$ splenic DCs are readily infected at this time (Figure 3). Consistent with a bone marrow specific defect in *Mbtps1*$^{wrt/wrt}$ mice, we also observed a loss of the usual conversion of granulocyte dominant to monocyte dominant bone marrow cells during LCMV Cl13 infection of *Mbtps1*$^{wrt/wrt}$ mice (Figure S2).

LCMV Cl13 Establishes Infection in *Mbtps1*$^{wrt/wrt}$ Spleen

Because splenic DC infection has been implicated as a critical factor for LCMV Cl13 persistence(Sevilla et al., 2004a), we hypothesized that with limiting amounts of Site 1 protease (S1P) there would be decreased virus production in splenic DC. However, instead we observed an increase in the number of DCs expressing the LCMV nucleoprotein (NP) in *Mbtps1*$^{wrt/wrt}$ (Figure 3AB). Although viral protein was abundant in *Mbtps1*$^{wrt/wrt}$ DC, we further sought to determine whether fully processed infectious virus might still be diminished. However, we observed that *Mbtps1*$^{wrt/wrt}$ DC indeed produced equivalent, if not more, cells containing infectious progeny than their WT counterparts (Figure 3). In contrast to reduced viral loads in the bone marrow compartment, neither *Mbtps1*$^{wrt/wrt}$ B or T lymphocytes, DC or bulk unsorted splenocytes showed diminished numbers of infectious centers. Therefore, the LCMV growth defect in *Mbtps1*$^{wrt/wrt}$ bone marrow is specific.

Mbtps1 Expression and Downstream Gene Expression is Decreased in *woodrat* Bone Marrow

Given the surprising finding that splenocytes supported productive viral replication, in striking contrast to cells from the bone marrow, we assessed the levels of *Mbtps1* expression as well as the genes it regulates in spleen, kidney, liver and bone marrow. We hypothesized that *Mbtps1* expression might be limited in the bone marrow. Therefore, further downregulation of *Mbtps1* in *wrt* would be insufficient for the critical amount of protease activity needed for a productive viral infection. Indeed, we observed a lower level of basal *Mbtps1* expression in the bone marrow as compared to other organs tested (Figure S3). This is consistent with a decreased level of *Mbtps1* expression in bone marrow as compared with almost all other organs as catalogued in both human and mice by BioGPS (Wu et al., 2009). As *Mbtps1* encodes a protease whose main function is to activate gene transcription programs, we also assessed for the levels of these target genes in spleen, kidney, liver and bone marrow. Consistent with decreased expression of *Mbtps1* in *wrt* bone marrow, we observed a decrease in *Mbtps1* regulated genes most dramatically in the bone marrow of *wrt* as compared to WT mice (Figure S3B). Interestingly, we observed an increase in expression of *Mbtps1* inducible genes in the spleen of *wrt* vs. WT (Figure S3B). This could contribute to the robust productive viral infection we observed in *wrt* splenocytes (Figure 2).

Defective LCMV Replication in bmDC but not bmMO or Primary Fibroblasts

As *Mbtps1*$^{wrt/wrt}$ monocytes and DCs exhibit specific resistance to LCMV Cl13 infection, we cultured bone marrow from *Mbtps1*$^{wrt/wrt}$ animals to investigate viral replication in two related professional antigen presenting cells (APCs), macrophages and DC, that are infected selectively by LCMV Cl13 (Matloubian et al., 1993; Sevilla et al., 2000; Sevilla et al., 2004a). We observed that viral growth kinetics in *Mbtps1*$^{wrt/wrt}$ bone-marrow derived macrophages as well as primary fibroblasts were essentially indistinguishable from WT in single and multistep growth curves (Figure 4AC). Consistent with unchanged viral growth kinetics, we observed efficient processing of LCMV GPC (Figure 4B). Occasionally, we have seen decreased total amounts of LCMV GPC in *Mbtps1*$^{wrt/wrt}$ primary fibroblasts. However we have never observed a defect in the processing of this protein. In contrast, LCMV replication was almost completely abrogated in *Mbtps1*$^{wrt/wrt}$ bone-marrow derived DC (bmDC) (Figure 4C).

woodrat Resistance is restricted by the S1P Cleavage Site

We hypothesized that diminished LCMV growth in bmDCs would map to ineffective S1P cleavage at position 270 after the amino acid recognition site, RRLA. Therefore, we utilized a previously characterized virus whereby the RRLA recognition sequence was replaced with the Furin recognition site RRRR (Rojek et al., 2010) referred to as “LCMV-Furin”. In

contrast to WT virus which requires S1P cleavage of viral GPC to complete its viral life cycle and is insensitive to Furin proteases, LCMV-Furin does not require S1P, but instead requires Furin to complete its life cycle (Rojek et al., 2010). We observed that LCMV-Furin grows with kinetics similar to LCMV-WT in WT bmDC, indicating that Furin is sufficient to replace the function of WT S1P, as indicated by prior studies (Rojek et al., 2010). Importantly, LCMV-Furin proliferated in *Mbtps1*$^{wrt/wrt}$ bmDC to an extent similar to its proliferation in *Mbtps1*$^{WT/WT}$ cells and the proliferation of WT virus in *Mbtps1*$^{WT/WT}$ cells (Figure 4D). Next we directly assessed the cleavage of GPC biochemically in *wrt* and WT bmDC. Consistent with our genetic experiment whereby the RRRR Furin recognition site was able to rescue viral growth in *wrt* bmDC (Figure 4D), we observed no processing of viral GPC to its cleavage products GP1 and GP2 in *wrt* bmDC(Figure 4E). Even with overexposure and/or overloading of protein, we were not able to detect any processing of GPC (Figure 4E, bottom panels).

In order to rule out other explanations for diminished viral production in *Mbtps1*$^{wrt/wrt}$ bmDCs we determined whether there was increased death of *Mbtps1*$^{wrt/wrt}$ bmDCs compared to WT bmDCs. We did not see a significant effect of the mutation on cell death (Figure S4ABC). In addition, we examined whether viral protein production might be diminished in *wrt* bmDCs to account for the decrease in infectious progeny. However, we did not observe any diminution in LCMV proteins in *Mbtps1*$^{wrt/wrt}$ bmDCs utilizing monoclonal antibodies against the nucleoprotein and glycoprotein or polysera against all LCMV antigens (Figure S4D, data not shown). Taken together, these data show failure of cleavage at the viral RRLA S1P recognition sequence within bmDCs as the mechanism for the genetic protection afforded by the hypomorphic *Mbtps1*^{wrt} allele.

Next we challenged *wrt* and WT mice with recombinant LCMV Cl13 viruses bearing either the native S1P or Furin recognition sequences. In contrast to our *ex vivo* experiments, the mutant Furin site altering amino acids 268 and 269 resulted in decreased viral fitness *in vivo.* However, consistent with our *ex vivo* findings, Cl13^{FURIN} produced significantly higher viral titers than the parent wildtype virus (Cl13^{S1P}) in *wrt* mice. Importantly, despite the attenuating effect of the Furin mutation in WT mice, this mutation demonstrated an increased fitness which was specific to *wrt* mice. We observed that Cl13^{S1P} was rapidly cleared in *wrt* vs. WT mice (similar to the passaged isolate), whereas Cl13^{FURIN} had equivalent (or better) replicative fitness in *wrt* vs. WT mice (consistent with our *ex vivo* bmDC findings). Furthermore, we sequenced virus from *wrt* animals to test whether the Furin mutation might not be tolerated *in vivo*. However, for both Cl13^{FURIN} and Cl13^{S1P} the GPC protease site was identical between the input and output viruses (data not shown), consistent with the selective advantage of the RRRR recognition site in *wrt* mice.

Adoptive Transfer of *woodrat* bmDC prevents persistent viral infection

Given our data regarding the potential contribution of bmDCs, we adoptively transferred *wrt* bmDCs to assess their ability to protect otherwise susceptible WT hosts. Consistent with our prior findings that implicated a role for DCs in persistent viral infection (Figures 2B, 4CD, and (Sevilla et al., 2000; Sevilla et al., 2003; Sevilla et al., 2004a)), we observed that *wrt* bmDCs alone were capable of conferring resistance to persistent viral infection (Figure 5A). Although the establishment of acute viremia was indistinguishable whether recipients received WT or *wrt* bmDC vs. vehicle, persistent viremia could only be qwelled with *wrt* bmDC immunotherapy. However, this effect was not seen when *wrt* bmDC were delivered after 2 days of infection (Figure S5A).

Previously, we have shown that Cl13 subverts DC function by inhibiting MHC and co-stimulatory molecules (Sevilla et al., 2004b). We hypothesized that *wrt* bmDC might be resistant to this viral subversion given the observed resistance to productive viral infection

(Figure 4C). This would result in an augmented adaptive immune response and therefore could provide an explanation for the kinetics of viral clearance seen with *wrt* bmDC immunotherapy. Flow cytometric analysis of bmDC infected *ex vivo* confirmed our prior findings that Cl13 infected DCs do not upregulate antigen presentation and co-stimulatory molecules as expected (Figure 5B). Surprisingly, *wrt* bmDC displayed augmented basal activation of MHC and co-stimulatory molecules. This activation was not significantly inhibited by Cl13 infection. However, this did not translate into increased T cell cytokine responses 7dpi (Figure S5B). Thus *wrt* DC might be acting as a sink for viral replication moreso than contributing to a greater inflammatory response.

DISCUSSION

These studies focused on the therapeutic target Site 1 Protease by utilizing the hypomorphic mutant *woodrat* to evaluate systemic S1P inhibition *in vivo*. As *Mbtps1*^{wrt} is the only viable animal model with systemic inhibition of S1P, this reagent provides a powerful means to assess the role of S1P inhibition *in vivo*. Therapeutically, Mbtps1 is an important potential target in the treatment of hypercholesterolemia and often fatal arenavirus infections. We directly assessed the role for this gene for both the acute and persistent variants of the prototypic arenavirus, LCMV.

Surprisingly, *in vivo* resistance in this model was observed mainly in chronic infection (Clone 13 infection), without a prominent role in acute infection (Armstrong infection). As expected, this hypomorphic mutation in a gene required for the viral life cycle does result in a decrease in viral titers. However, this decrease is organ and cell type specific. Our interpretation of these data is that persistent viral infection requires infection and viral subversion of specific cell types which are genetically resistant to infection in *Mbtps1*^{wrt}(i.e. bone marrow cells including monocytes and DCs), implicating an important role for these cell types in persistent versus acute infections. We believe these cells might be more sensitive to the *wrt* mutation (in contrast to splenocytes or hepatocytes) due to a lower level of S1P activity in cells from the bone marrow. Indeed, we observed lower expression of both *Mbtps1* as well as downstream target genes in bone marrow as compared to other compartments. Given the hypomorphic activity of *Mbtps1* in *wrt*, this would further decrease *Mbtps1* function below a potentially critical threshold necessary for a productive viral infection in the bone marrow.

In order to confirm the mechanism of protection in *wrt*, we applied a genetic test, host complementation. In this test, mutation of the viral proteolytic recognition sequence for *Mbtps1*,RRLA to RRRR which can be recognized by the ubiquitous protease Furin, should restore viral fitness in the *wrt* host. This restoration of viral replication should be specific to mutations in both the host and viral genes involved. Consistent with this reasoning, we observed specific rescue of Cl13^{FURIN} viral replication in *wrt* bmDC. Moreover, complementation was also observed *in vivo*. Cl13^{FURIN} had increased viral fitness in *wrt* as compared to otherwise more susceptible WT mice. Of note, it remains unclear why Cl13^{FURIN} is ultimately attenuated *in vivo*. We have observed many times prior that various engineered viruses which we have produced display severe *in vivo* attenuation which was not seen *in vitro* (unpublished observations, (Emonet et al., 2009)). We suspect that the numerous differences in cell type and extracellular milieu *in vivo* vs. *in vitro* contribute to this phenomenon. Importantly, our observations were specific to the proteolytic cleavage site in the LCMV GPC and the cognate mutation in the protease *Mbtps1*. Although the 2 amino acid changes in Cl13^{FURIN} attenuate the virus *in vivo* in an unknown manner, the selective advantage offered by complementing viral proteolytic cleavage with Furin outweighs the cost of utilizing the mutant RRRR site. We confirmed this by directly sequencing viral GPC 5dpi from serum. In all cases we observed no deviation from the

engineered protease target sequences in output virus as compared to the sequence in the inoculating virus. Importantly, maintenance of the RRRR recognition site in *wrt* serum is despite normal processing in several cell types as well as equivalent productive infection in organs (i.e. spleen and liver) at this time in *wrt* as compared to WT mice. Importantly, these findings offer insight towards the importance of cell type specificity when targeting viral processing activity. This is imminently important for HIV/AIDS research regarding protease inhibitors in clinical use.

These studies highlight the importance of studying genes systemically *in vivo* utilizing a hypomorphic mutation when null mutations are non-viable. In this way, one can compare the relative roles of different cell types in a physiologically relevant situation where a therapeutic target is partially inhibited. When limited to complete nulls many therapeutic targets can no longer be studied secondary to embryonic lethality. In addition, complete target inhibition is physiologically unlikely in real-world settings.

Utilizing *wrt* mice in this study we have uncovered two key findings regarding therapeutic targeting of S1P: inhibition of S1P function results is host lymphocyte immunodeficiency and inhibition of S1P is a therapeutically viable option for treatment of persistent arenavirus infection *in vivo.* These findings are important given the potential therapeutic role of S1P inhibition for treatment of hypercholesterolemia and often fatal arenavirus infections (Hawkins et al., 2008; Hay et al., 2007). Understanding the consequences of systemic inhibition of this therapeutic target is critical in determining its clinical utility.

Regarding our understanding of persistent viral infection, analysis of the *wrt* mutation has demonstrated two critical findings—the role of cell type specificity in controlling persistent viral infection and the potential therapeutic utility of bmDCs in protection from persistent viral infection.

We have found cell type specific resistance to viral growth in bmDC. In response to this finding as well as growing literature supporting the central role of DC in persistent viral infections and tumor immune escape (Chaput et al., 2008; Liu et al., 2009; Oldstone, 2009; Zwirner et al., 2010), we tested the therapeutic role of bmDC that are genetically resistant to LCMV challenge. We believe *wrt* bmDC are therapeutic in contrast to WT bmDC for two reasons. Firstly, DC express a high level of the arenavirus receptor alpha-dystroglycan (unpublished observations), but after viral entry this becomes a dead end for viral replication in *wrt* bmDC, effectively a sink for infectious virus particles. Secondly, we observed basal activation in *wrt* bmDC which is not inhibited by Cl13 infection. Being a critical cell type in persistent viral infections this may also contribute to host protection, although as we did not observe augmentation in virus specific peptide stimulation 7dpi, this appears to play a smaller role, if any.

Our results raise an important consideration when transferring DCs therapeutically into patients. There has been much speculation and experimentation in further supplementing a host with DC to combat both infectious and oncologic diseases(Ilett et al., 2010; Lehman et al., 2010). Our data highlights that simply boosting the levels of these central immune sentinels may not be sufficient to clear a pathogenic challenge. This is likely secondary to the numerous subversive tactics already in place compromising the host immune response. Rather, optimizing this cell type to resist infectious or oncologic countermeasures, as in our model, may be critical to fully utilize DC and other immune cell types to advance the field of immunotherapy.

EXPERIMENTAL PROCEDURES

Mice and viruses

C57BL/6J mice were from the Rodent Breeding Colony at The Scripps Research Institute. C57BL/6J mice were used for ENU mutagenesis to generate the *woodrat* strain, as described at http://mutagenetix.scripps.edu.

All mice were housed under specific pathogen–free conditions. Mouse handling conformed to the requirements of the National Institutes of Health and The Scripps Research Institute Animal Research Committee. Mice were infected intravenously with 2×10^6 PFU of LCMV-Arm or LCMV-Cl 13. To test immunologic memory and protection, mice were rechallenged intravenously with 2×10^6 PFU of LCMV-Cl 13. Viral stocks were prepared and viral titers were measured as previously described(Evans et al., 1994).

Cell isolation

Total splenic DCs (CD45+CD3−NK1.1−CD19−CD11c+), B cells (CD45+CD3−NK1.1−CD11c−CD19+) and T cells (CD45+CD3+NK1.1−CD11c−CD19−) were sorted using a FACSVantage fluorescence activated cell sorter (Becton Dickinson) as previously described(Zuniga et al., 2004). Purities for all populations after sorting were >99%.

Intracellular cytokine analysis and flow cytometry

Splenocytes were stimulated for 5 h with 5 mg/ml of the MHC class II–restricted LCMV GP61–80 or 2 mg/ml of the MHC class I–restricted LCMV NP396–404 or GP33–41 (all >99% pure; Peprotech) in the presence of 50 U/ml recombinant murine IL-2 (Peprotech) and 1 mg/ml brefeldin A (BD Pharmingen). Addition of IL-2 to the *ex vivo* stimulation did not alter cytokine production (data not shown). Cells were stained for surface expression of CD4 (clone RM4-5, Pharmingen) and CD8 (clone 53–6.7, Caltag). Cells were fixed, permeabilized and stained with antibodies to TNF-α (clone MP6-XT22), IFN-g (clone XMG1.2), IL-2 (clone JES6-5H4). Flow cytometric analysis was performed using a Digital LSR II (Becton Dickinson). MHC class I and class II tetramers were produced and used for staining as previously described(Homann et al., 2001).

Immunofluorescent microscopy

Three-color images were collected with an Axiovert S100 immunofluorescence microscope(Zeiss) fitted with an automated xy stage and a Axiocam color digital camera. To obtain tissues, organs were removed and frozen in OCT and 6-mm frozen sections were cut and stained overnight at 4°C with a guinea pig polysera to LCMV (1:2,000 dilution), NP113 mouse monoclonal specific for LCMV NP, 83.6 mouse monoclonal specific for LCMV GP and/or ER-TR7 rat monoclonal (Abcam) (all at 1ug/mL final concentration). Tissues or 96-well plate bound cells were washed and incubated at 4°C for 3h with species specific secondary antibodies, washed and incubated with 4,6-diamidino-2-phenylindole (DAPI, 1 mg/ml) prior to imaging.

51Cr release assays

In vitro 51Cr release assays were performed on day 9 after infection. MC57 target cells were labeled with 1 mg/ml LCMV GP33–41 or NP396–404 peptides or left unlabeled, and then mixed with splenocytes at a 50:1 effector/target ratio. Samples were performed in triplicate and 51Cr release was measured in the supernatant after 5h as previously described(Borrow et al., 1995).

DNA Transfection and Rescue of LCMV from Cloned cDNAs

Virus rescue was done as described previously(Flatz et al., 2006). Subconfluent BHK-21 cells (2 × 106 cells per M6 well) were transfected for 5 h by using 2.5 μL of Lipofectamine 2000 (Invitrogen) per microgram of plasmid DNA. The RRLA site naturally found in LCMV Clone13 GPC sequence was changed to the Furin recognition site, RRRR, by site-directed mutagenesis.

RNA Preparation and Sequencing

RNA was extracted from serum 5 dpi by using TRI reagent (Molecular Research Center). Reverse-transcription reaction was done with the Masterscript kit (5 PRIME) and primers specific for LCMV GPC. PCR amplified products were directly sequenced.

Western Blot Analysis

Cell homogenate was collected with Laemmli buffer as described previously(Popkin et al., 2003). Protein content was determined by BCA assay (Pierce), and protein samples were analyzed by reducing 4–12% SDS/PAGE (Nupage Bis-Tris-Gel; Invitrogen) and were detected using three monoclonal antibodies 83.6, WE-33.1, WE36.1 (all anti-LCMV GP(Buchmeier et al., 1981)) and anti-actin or tubulin (Sigma) antibodies as loading controls.

Generation of BM Chimeric Mice

Generation of BM chimeric mice was performed as described(Brandl et al., 2009). Recipient WT (CD45.1) or Mbtps1wrt/wrt (CD45.2) mice were lethally irradiated with 950 rad using a 137Cs source and injected intravenously 3 h later with 5×10^6 BM cells derived from the tibia and femurs of the respective donors. Six to eight weeks after engrafting, reconstitution was assessed by FACS analysis of bone marrow and/or peripheral blood cells. After red blood cell lysis, cells were stained with FITC-labeled CD45.1 antibody and PerCPCy5.5-labeled CD45.2 antibody. All animals had >99% hematopoietic cells of donor origin.

Bone marrow culture of professional antigen presenting cells

Bone marrow was harvested and cultured as described previously(Liou et al., 2008; Popkin et al., 2003). GM-CSF or M-CSF(Peprotech) were kept in culture media (both at 10ng/mL final) for bmDC or bmMO, respectively, during the entire course of experiments. bmAPC were used at 6 days post *ex vivo* culture or as stated.

qRT-PCR

RNA (1.0 μg) was reverse transcribed by using random hexamers and 18-dT and SuperScript II (Invitrogen). One one-hundredth of this product was PCR amplified, and incorporation of SYBR green (Molecular Probes) was quantified. All PCR reactions (primers obtained from OriGene) were performed in triplicate for each experiment. 18S normalized data were used to quantitate relative levels of gene expression by using ΔΔCt analysis.

Adoptive transfer

bmDC were cultured as above and 6 million cells or PBS vehicle control were transferred on day 6 of culture into recipient C57BL/6J mice.

Statistical analysis

Statistical analysis was performed on Prism software. All P-values <0.05 were considered significant. Error bars denote the standard error of the mean (SEM). *= P-value <0.05; **= P-value <0.005.

Supplementary Material

Refer to Web version on PubMed Central for supplementary material.

Acknowledgments

This is Publication 20942 from the Departments of Immunology and Microbial Science and Genetics, The Scripps Research Institute, La Jolla, CA. Our work was supported by National Institutes of Health Grants as followed: Training Grant AI007244 (to D.L.P.), AI070167 (to B.B.) and AI09484, AI70967 (to M.B.A.O).

References

Bergeron E, Vincent M, Nichol S. Crimean-Congo hemorrhagic fever virus glycoprotein processing by the endoprotease SKI-1/S1P is critical for virus infectivity. J Virol 2007;81:13271–13276. [PubMed: 17898072]

Borrow P, Evans C, Oldstone M. Virus-induced immunosuppression: immune system-mediated destruction of virus-infected dendritic cells results in generalized immune suppression. J Virol 1995;69:1059–1070. [PubMed: 7815484]

Brandl K, Rutschmann S, Li X, Du X, Xiao N, Schnabl B, Brenner D, Beutler B. Enhanced sensitivity to DSS colitis caused by a hypomorphic Mbtps1 mutation disrupting the ATF6-driven unfolded protein response. Proc Natl Acad Sci U S A 2009;106:3300–3305. [PubMed: 19202076]

Brown MS, Ye J, Rawson RB, Goldstein JL. Regulated intramembrane proteolysis: a control mechanism conserved from bacteria to humans. Cell 2000;100:391–398. [PubMed: 10693756]

Buchmeier MJ, Lewicki HA, Tomori O, Oldstone MB. Monoclonal antibodies to lymphocytic choriomeningitis and pichinde viruses: generation, characterization, and cross-reactivity with other arenaviruses. Virology 1981;113:73–85. [PubMed: 6267791]

Bukrinsky M, Sviridov D. Human immunodeficiency virus infection and macrophage cholesterol metabolism. J Leukoc Biol 2006;80:1044–1051. [PubMed: 17056763]

Carter C, Onafuwa-Nuga A, McNamara L, Riddell Jt, Bixby D, Savona M, Collins K. HIV-1 infects multipotent progenitor cells causing cell death and establishing latent cellular reservoirs. Nat Med 2010;16:446–451. [PubMed: 20208541]

Chaput N, Conforti R, Viaud S, Spatz A, Zitvogel L. The Janus face of dendritic cells in cancer. Oncogene 2008;27:5920–5931. [PubMed: 18836473]

Chen X, Shen J, Prywes R. The luminal domain of ATF6 senses endoplasmic reticulum (ER) stress and causes translocation of ATF6 from the ER to the Golgi. J Biol Chem 2002;277:13045–13052. [PubMed: 11821395]

de la Torre JC, Oldstone MB. Anatomy of viral persistence: mechanisms of persistence and associated disease. Adv Virus Res 1996;46:311–343. [PubMed: 8824703]

Emonet SF, Garidou L, McGavern DB, de la Torre JC. Generation of recombinant lymphocytic choriomeningitis viruses with trisegmented genomes stably expressing two additional genes of interest. Proc Natl Acad Sci U S A 2009;106:3473–3478. [PubMed: 19208813]

Evans C, Borrow P, de la Torre J, Oldstone M. Virus-induced immunosuppression: kinetic analysis of the selection of a mutation associated with viral persistence. J Virol 1994;68:7367–7373. [PubMed: 7933120]

Flatz L, Bergthaler A, de la Torre JC, Pinschewer DD. Recovery of an arenavirus entirely from RNA polymerase I/II-driven cDNA. Proc Natl Acad Sci U S A 2006;103:4663–4668. [PubMed: 16537369]

Hawkins J, Robbins M, Warren L, Xia D, Petras S, Valentine J, Varghese A, Wang I, Subashi T, Shelly L, et al. Pharmacologic inhibition of site 1 protease activity inhibits sterol regulatory element-binding protein processing and reduces lipogenic enzyme gene expression and lipid synthesis in cultured cells and experimental animals. J Pharmacol Exp Ther 2008;326:801–808. [PubMed: 18577702]

Hay B, Abrams B, Zumbrunn A, Valentine J, Warren L, Petras S, Shelly L, Xia A, Varghese A, Hawkins J, et al. Aminopyrrolidineamide inhibitors of site-1 protease. Bioorg Med Chem Lett 2007;17:4411–4414. [PubMed: 17583500]

Homann D, Teyton L, Oldstone M. Differential regulation of antiviral T-cell immunity results in stable CD8+ but declining CD4+ T-cell memory. Nat Med 2001;7:913–919. [PubMed: 11479623]

Ilett E, Prestwich R, Melcher A. The evolving role of dendritic cells in cancer therapy. Expert Opin Biol Ther 2010;10:369–379. [PubMed: 20132058]

Jamieson B, Butler L, Ahmed R. Effective clearance of a persistent viral infection requires cooperation between virus-specific Lyt2+ T cells and nonspecific bone marrow-derived cells. J Virol 1987;61:3930–3937. [PubMed: 3500329]

Lehman T, O'Halloran K, Hoover E, Avery P. Utilizing the FIV model to understand dendritic cell dysfunction and the potential role of dendritic cell immunization in HIV infection. Vet Immunol Immunopathol 2010;134:75–81. [PubMed: 19896214]

Li Q, Skinner P, Ha S, Duan L, Mattila T, Hage A, White C, Barber D, O'Mara L, Southern P, et al. Visualizing antigen-specific and infected cells in situ predicts outcomes in early viral infection. Science 2009;323:1726–1729. [PubMed: 19325114]

Liou L, Blasius A, Welch M, Colonna M, Oldstone M, Zuniga E. In vivo conversion of BM plasmacytoid DC into CD11b+ conventional DC during virus infection. Eur J Immunol 2008;38:3388–3394. [PubMed: 18979509]

Liu B, Woltman A, Janssen H, Boonstra A. Modulation of dendritic cell function by persistent viruses. J Leukoc Biol 2009;85:205–214. [PubMed: 18818373]

Matloubian M, Kolhekar S, Somasundaram T, Ahmed R. Molecular determinants of macrophage tropism and viral persistence: importance of single amino acid changes in the polymerase and glycoprotein of lymphocytic choriomeningitis virus. J Virol 1993;67:7340–7349. [PubMed: 7693969]

Nadanaka S, Yoshida H, Kano F, Murata M, Mori K. Activation of mammalian unfolded protein response is compatible with the quality control system operating in the endoplasmic reticulum. Mol Biol Cell 2004;15:2537–2548. [PubMed: 15020717]

Oldstone M. Anatomy of viral persistence. PLoS Pathog 2009;5:e1000523. [PubMed: 19649277]

Oldstone MB. Arenaviruses. II. The molecular pathogenesis of arenavirus infections. Introduction Curr Top Microbiol Immunol 2002;263:V–XII.

Popkin D, Watson M, Karaskov E, Dunn G, Bremner R, Virgin Ht. Murine cytomegalovirus paralyzes macrophages by blocking IFN gamma-induced promoter assembly. Proc Natl Acad Sci U S A 2003;100:14309–14314. [PubMed: 14614150]

Recher M, Lang KS, Navarini A, Hunziker L, Lang PA, Fink K, Freigang S, Georgiev P, Hangartner L, Zellweger R, et al. Extralymphatic virus sanctuaries as a consequence of potent T-cell activation. Nat Med 2007;13:1316–1323. [PubMed: 17982463]

Riethmüller J, Riehle A, Grassmé H, Gulbins E. Membrane rafts in host-pathogen interactions. Biochim Biophys Acta 2006;1758:2139–2147. [PubMed: 17094939]

Rojek J, Kunz S. Cell entry by human pathogenic arenaviruses. Cell Microbiol 2008;10:828–835. [PubMed: 18182084]

Rojek J, Pasqual G, Sanchez A, Nguyen N, de la Torre J, Kunz S. Targeting the proteolytic processing of the viral glycoprotein precursor is a promising novel antiviral strategy against arenaviruses. J Virol 2010;84:573–584. [PubMed: 19846507]

Rojek J, Perez M, Kunz S. Cellular entry of lymphocytic choriomeningitis virus. J Virol 2008;82:1505–1517. [PubMed: 18045945]

Ron D, Walter P. Signal integration in the endoplasmic reticulum unfolded protein response. Nat Rev Mol Cell Biol 2007;8:519–529. [PubMed: 17565364]

Sevilla N, Kunz S, Holz A, Lewicki H, Homann D, Yamada H, Campbell K, de La Torre J, Oldstone M. Immunosuppression and resultant viral persistence by specific viral targeting of dendritic cells. J Exp Med 2000;192:1249–1260. [PubMed: 11067874]

Sevilla N, Kunz S, McGavern D, Oldstone M. Infection of dendritic cells by lymphocytic choriomeningitis virus. Curr Top Microbiol Immunol 2003;276:125–144. [PubMed: 12797446]

Sevilla N, McGavern D, Teng C, Kunz S, Oldstone M. Viral targeting of hematopoietic progenitors and inhibition of DC maturation as a dual strategy for immune subversion. J Clin Invest 2004a; 113:737–745. [PubMed: 14991072]

Sevilla N, McGavern DB, Teng C, Kunz S, Oldstone MB. Viral targeting of hematopoietic progenitors and inhibition of DC maturation as a dual strategy for immune subversion. J Clin Invest 2004b; 113:737–745. [PubMed: 14991072]

van der Most R, Sette A, Oseroff C, Alexander J, Murali-Krishna K, Lau L, Southwood S, Sidney J, Chesnut R, Matloubian M, et al. Analysis of cytotoxic T cell responses to dominant and subdominant epitopes during acute and chronic lymphocytic choriomeningitis virus infection. J Immunol 1996;157:5543–5554. [PubMed: 8955205]

Wu C, Orozco C, Boyer J, Leglise M, Goodale J, Batalov S, Hodge CL, Haase J, Janes J, Huss JW 3rd, et al. BioGPS: an extensible and customizable portal for querying and organizing gene annotation resources. Genome Biol 2009;10:R130. [PubMed: 19919682]

Yang J, Goldstein J, Hammer R, Moon Y, Brown M, Horton J. Decreased lipid synthesis in livers of mice with disrupted Site-1 protease gene. Proc Natl Acad Sci U S A 2001;98:13607–13612. [PubMed: 11717426]

Ye J, Rawson RB, Komuro R, Chen X, Dave UP, Prywes R, Brown MS, Goldstein JL. ER stress induces cleavage of membrane-bound ATF6 by the same proteases that process SREBPs. Mol Cell 2000;6:1355–1364. [PubMed: 11163209]

Zuniga E, McGavern D, Pruneda-Paz J, Teng C, Oldstone M. Bone marrow plasmacytoid dendritic cells can differentiate into myeloid dendritic cells upon virus infection. Nat Immunol 2004;5:1227–1234. [PubMed: 15531885]

Zwirner N, Croci D, Domaica C, Rabinovich G. Overcoming the hurdles of tumor immunity by targeting regulatory pathways in innate and adaptive immune cells. Curr Pharm Des 2010;16:255–267. [PubMed: 20109135]

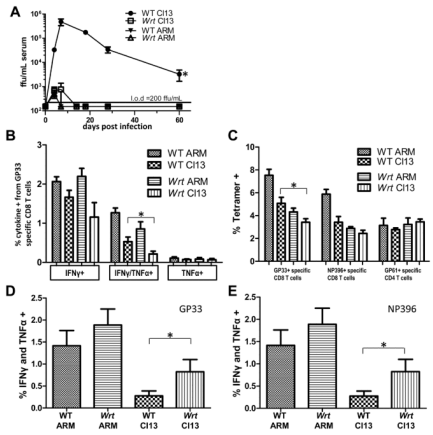

Figure 1. *Mbtps1*^{wrt} *(wrt)* are resistant to LCMV Cl13 infection despite immunodeficiency

A) *Mbtps1*^{wrt} are resistant to persistent LCMV Cl13 infection but the kinetics of viremia are not altered during infection with the acute LCMV Armstrong (ARM) parent strain. Mean and SEM are shown from 6–12 mice/group at the indicated times post infection. B) GP33 *ex vivo* peptide stimulation and C) viral peptide specific T cell enumeration with tetramers from splenocytes 5dpi. D) *Mbtps1*^{wrt} mount a CTL immune response to LCMV Cl13, 9 dpi, when WT CTL exhibit exhaustion. GP33 and E) NP396 *ex vivo* peptide stimulation from splenocytes. Mean and SEM are shown from 6 mice/group. *=P-value<0.05. **=P-value<0.005.

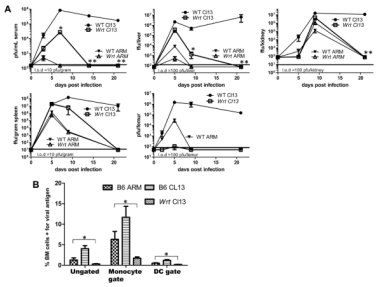

Figure 2. *Mbtps1*^{wrt} are susceptible to establishment of LCMV Cl13 infection in serum, spleen, liver and kidney, but have an early sustained defect in the bone marrow

A) *Mbtps1*^{wrt} are susceptible to LCMV Cl13 replication in serum, spleen, liver and kidney. Mean and SEM are shown from 4–6 mice/group at the indicated times post infection. B) In the bone marrow, monocytes and DC have defective establishment of LCMV Cl13 in *Mbtps1*^{wrt}. Mean and SEM are shown from 5 mice/group, 5 dpi. *=P-value<0.05. **=P-value<0.005.

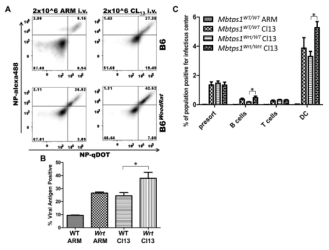

Figure 3. *Mbtps1*^{wrt} splenic DC are susceptible to LCMV Cl13 infection

A) Splenocytes were stained for the intracellular viral antigen NP conjugated to qDot655 and alexa488. Gated DCs shown were CD11c+, NK1.1−, CD3−. Flow cytometry dataset is summarized in B. B) Mean and SEM from 6 mice are shown. C) Splenocytes were sorted for B, T and dendritic cells. Cells bearing infectious virus were quantitated by infectious center assay. All mice were analyzed 9 dpi. Mean and SEM from 6 mice are shown. *=P-value<0.05. **=P-value<0.005.

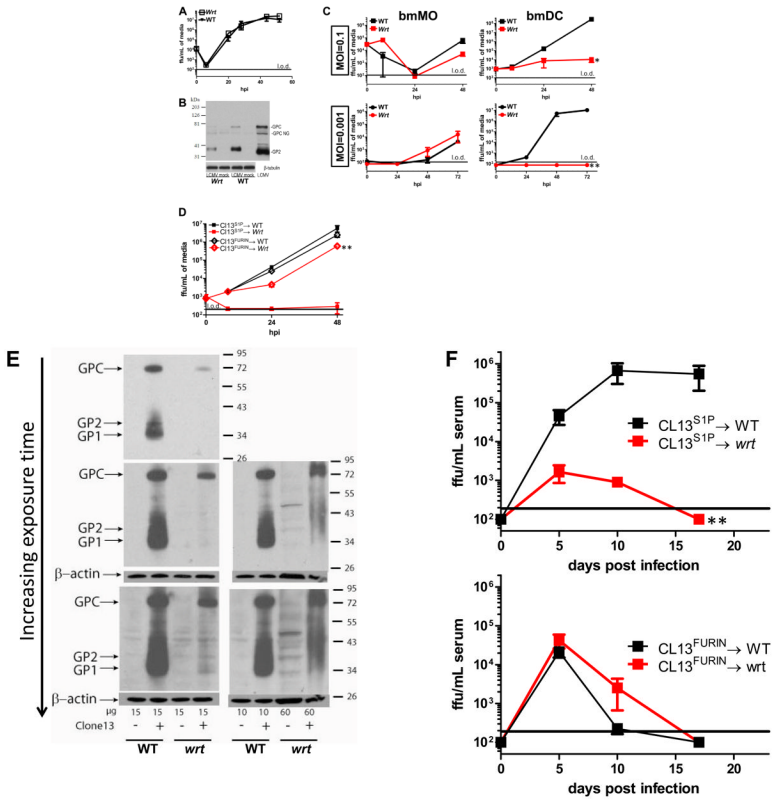

Figure 4. *Mbtps1*^{wrt} fibroblasts and macrophages support viral growth in contrast to dendritic cells in which viral growth is restricted by the S1P cleavage site, RRLA

A) *Ex vivo* multistep LCMV Cl13 growth curves in *wrt* vs. WT primary fibroblasts. Mean and SEM are shown for one of 2 similar independent experiments (N=4). B) Western blot of LCMV GP from *wrt* and WT primary fibroblasts. GPC, GPC non glycosylated (NG) and processed GP2 are visualized with the monoclonal antibody 83.6. Concentrated LCMV stock was used as a positive control. N=3. C) *Ex vivo* LCMV Cl13 growth curves in *wrt* vs. WT primary bone-marrow derived macrophages and dendritic cells (bmMO and bmDC, respectively). Cells were inoculated at a multiplicity of infection (MOI) of 0.1 and 0.001 as shown. Mean and SEM of viral titers are shown for one of 2 similar independent experiments (N=4). D) *Ex vivo* LCMV growth curves in *wrt* vs. WT bmDC with recombinant virus containing the native LCMV Mbtps1 cleavage site (RRLA), designated S1P, vs. the Furin protease cleavage site (RRRR) in lieu of RRLA, designated FURIN. MOI=0.1. Similar results were seen using either the Armstrong or Cl13 viral backbones. Mean and SEM of viral titers are shown for one of 2 similar independent experiments (N=4). E) Western blot of LCMV GP from *wrt* and WT bmDC. Lysates were collected 24hpi and blotted for GPC and its cleavage products GP1 and GP2. One of 3 experiments is shown. F) Recombinant viruses containing either the native S1P cleavage site, RRLA, or the Furin recognition site, RRRR, were used to infect *wrt* and WT mice. Mice were bled on the indicated days post infection and titered for infectious virus. Mean and SEM of viral titers are shown for one of 2 similar independent experiments (N=4). Of note, Cl13^{FURIN} serum levels were significantly higher at 5dpi in *wrt* mice as compared to the parent virus, Cl13^{S1P} in *wrt*. *=P-value<0.05. **=P-value<0.005.

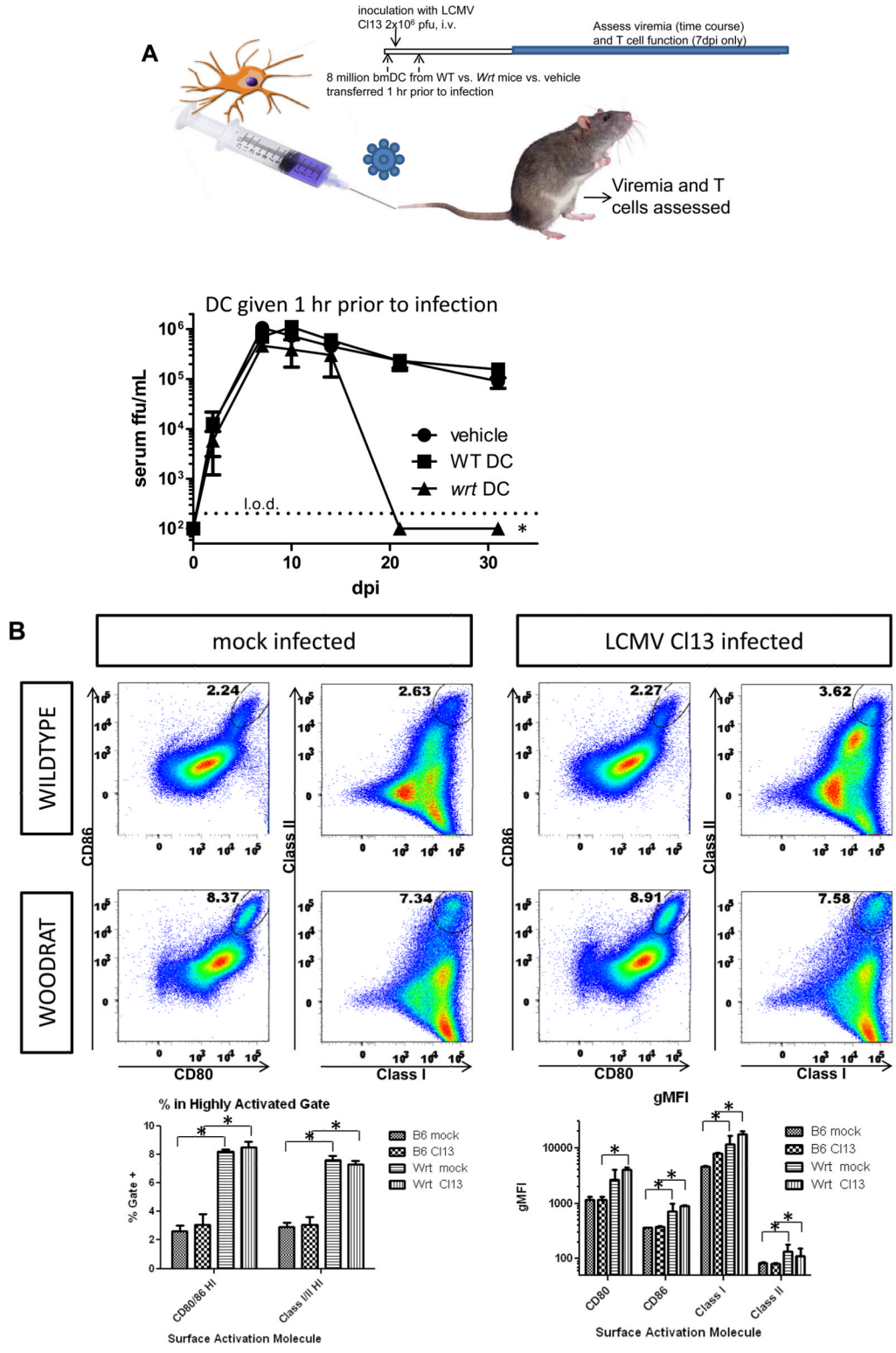

Figure 5. Adoptive immunotherapy with *Mbtps1*^{wrt} *bm*DC eliminates viral persistence

A) bmDC were cultured from WT and *wrt* mice. Eight million bmDC were adoptively transferred i.v. into 8–10wk old recipient WT B6 mice. Either 1 hour after, or 2 days prior to

infection with 2×10^6 pfu LCMV Cl13, bmDC were adoptively transfered to recipient B6 mice. Serum was harvested and titered at the indicated times. Mean and SEM from 8 mice/group are shown. B) *wrt* bmDC have higher levels of MHC molecules (class I and class II) and costimulatory molecules (CD80 and CD86). Flow cytometric analysis of bmDC from WT and *wrt* mice are shown with Mean and SEM for both % of cells in highly activated gate as well as gMFI for MHC and costimulatory molecules from one of 2 similar independent experiments (N=4). *=P-value<0.05.

Table 1

***Mbtps1*^{wrt} are immunodeficient when challenged with LCMV Armstrong**

Diet and dpi are indicated for *ex vivo* peptide stimulation assay, cytotoxic killing assay and anti-LCMV antibody titers.

Diet	Parameter	*Mbtps1* $^{WT/WT}$	*Mbtps1* $^{Wrt/WT}$	*Mbtps1* $^{Wrt/Wrt}$	*Mbtps1*$^{Wrt/Wrt}$ + 5% + cholesterol diet
Primary response					
Regular	7dpi %IFNγ$^+$np396$^+$CD8$^+$	**6±1**	7±3	**0.4±3**	n.d.*
	7dpi %IFNγ$^+$gp33$^+$CD8$^+$	**2±1**	2±0.6	**0.4±0.2**	n.d.*
Cholesterol	7dpi specific cytotoxic activity	n.d.	**57**	**8**	39*
	28dpi anti-LCMV antibodies	n.d.	**860**	**263**	643*
Secondary response					
Regular	74dpi %IFNγ$^+$np396$^+$CD8$^+$	5±1	12±3	7±0.2	n.d.
	74dpi %IFNγ$^+$gp33$^+$CD8$^+$	4±0.8	5±0.4	4±1	n.d.

*P-value<0.05.